Supporting Online Material for

WNT and DKK Determine Hair Follicle Spacing Through a Reaction-Diffusion Mechanism

Stefanie Sick, Stefan Reinker, Jens Timmer, Thomas Schlake*

*To whom correspondence should be addressed. E-mail: schlake@immunbio.mpg.de

This PDF file includes

Materials and Methods
SOM Text
Figs. S1 to S6
References

Supporting Online Material

Material and Methods
1. Modeling
In order to account for the characteristics of the WNT signaling pathway, we modified the Gierer-Meinhardt equations that take the form

$$\frac{\partial a}{\partial t} = D_a \Delta\, a + \rho_a F(a,h) - \mu_a a,$$

$$\frac{\partial h}{\partial t} = D_h \Delta\, h + \rho_h F(a,h) - \mu_h h.$$

Here, a and h describe the time and space dependent concentrations of the activator and inhibitor. Both substances diffuse, react with each other, and decay. The diffusion constants for the activator, D_a, and inhibitor, D_h, describe the speed of diffusion, which depends on the Laplacian (Δ) of the concentration profile. Reactions between the activator and inhibitor substances are determined by the $F(a,h)$ term. The reaction constants ρ_a and ρ_h scale the speed of the reactions. Additionally, both substances are removed linearly from the system with decay constants μ_a and μ_h. Conditions for the emergence of patterns in this model system are that the inhibitor diffuses more rapidly than the activator, that is $D_a \ll D_h$, and that the inhibitor adapts rapidly to changes of the activator, which is the case if it decays more rapidly than the activator, that is $\mu_a < \mu_h$ (*1*).

WNT receptor binding evokes production of both itself and DKK, so that we take the production term F to be the same in both equations (in contrast to the standard Gierer-Meinhardt model). In order to reflect the inhibitory action of DKK on WNT which takes place at the LRP co-receptor (*2*), the influence of h takes the form for non-competitive inhibition (*3*). We also included a saturation of the production speed with a Hill term. Then

$$F(a,h) = \frac{a^2}{(K_h + h)(1 + \kappa a^2)}.$$

As parameter values we chose $D_a = 0.005$, $D_h = 0.2$, $\rho_a = 0.005$ $\rho_h = 0.02$, $\mu_a = 0.005$, $\mu_h = 0.015$, $K_h = 0.1$, and $\kappa = 0.01$. Here it should be noted that the actual parameter values are arbitrary and not based on experimentally measured quantities. However, the system is robust to parameter variations and the actual values do not affect the qualitative behavior of the system. In fact, in reaction-diffusion equations a non-dimensionalization and rescaling of time and space can transform one pattern density into another (*4*).

We performed simulations of our model on a square grid with a standard partial differential equation solver from the NAG libraries which uses the method of lines (d03rafe). Initial conditions at each point in space were drawn from a normal distribution centered on the steady state and at the boundaries we imposed von Neumann conditions.

In order to model consecutive waves of hair follicle formation in mouse skin, we fixed the spots from the first simulation by adding a constant activator and inhibitor production at locations where a was above a threshold of 2. In the second wave where we doubled the size of the system by stretching the coordinates to the increased area to reflect embryo growth during development, the locations of first wave follicles additionally produce activator and inhibitor at constant rates of 0.005 and 0.01, respectively. To simulate that follicles of the first inductive wave are insensitive to activator and inhibitor during a subsequent wave, ρ_a and ρ_h were set to 0 at these locations.

In order to simulate the effects of an altered production of activator and inhibitor, respectively, values for ρ_a and ρ_h were increased/decreased. Changes in inhibitor decay were accounted for by increasing/decreasing μ_h.

2. Mice, Generation of transgenic mice

BATgal mice have been previously described (*5*). The coding regions of *Dkk2* and *Dkk4* were amplified by PCR of P10 cDNA from skin using the following primers which contain *Not*I sites for subcloning: 5'-GATGCGGCCGCCATGGCCGCGCTGATGCGGGTC-3' and 5'-GATGCGGCCGCTCAGATCTTCTGGCATACATGG-3' for *Dkk2*; 5'-GATGCGGCCGCGAGAGACCAGAGTGACTGAG-3' and 5'-GATGCGGCCGCAGGGCTACACAGTGAGATCC-3' for *Dkk4*. *Dkk1* (a kind gift of C. Niehrs), *Dkk2* and *Dkk4* cDNAs were cloned into an expression vector containing a 30 kb promoter fragment of the *Foxn1* gene (*6*). The transgenes were released by digestion with *Sal*I and microinjected into fertilized eggs from FVB mice. Founder mice were backcrossed to BALB/c mice.

3. Histology, In situ hybridization

Back skin from murine embryos and born mice of various ages was fixed in 4% paraformaldehyde, paraffin embedded, and sectioned at 6 µm for hematoxylin and eosin staining or in situ hybridization. Essentially, non-radioactive in situ hybridizations were performed as previously described (*7*). Both sense and antisense strands of gene-specific fragments were used as probes. These fragments were generated by PCR using the following gene-specific primers (fragment size is indicated): *Dkk1*: nt. 105-124 and nt. 927-946 in NM_010051 (842 bp); *Dkk2*: nt. 743-763 and nt. 1501-1520 in NM_020265 (778 bp); *Dkk4*: nt. 120-139 and nt. 899-918 in NM_145592 (799 bp).

4. Transactivation experiments

To obtain pGL3-Dkk4, a 700 bp murine *Dkk4* promoter fragment was amplified by PCR using the following primers containing either a *BamH*I or a *Hind*III site for cloning into the promoter-less pGL3-Basic (Promega) luciferase reporter construct: 5'-ACTGGATCCACACACTGGAACTGCAGGTG-3' and 5'-CAGACAAGCTTTAAATGAGACAGGCCAGGTC-3'. pGL3-Dkk4mut was generated from pGL3-Dkk4 by PCR-based mutagenesis that destroyed all five LEF/TCF consensus binding sites by converting the two nucleotides upstream of the 5'-CAAAG-3' motif into 5'-GC-3'. Each luciferase reporter plasmid was cotransfected with a β-galactosidase expression construct, pBOS-βgal (*8*), and with either empty vector or expression plasmids for β-catenin and *Lef1* into HEK293 cells by calcium phosphate coprecipitation. Twenty-four hours after transfection, the $CaPO_4$ precipitate was washed away from the cells, and fresh medium was added for another 24 hr. The cells were then harvested into 250 mM TrisHCl (pH 7.5) buffer and disrupted by three freeze-thaw cycles. The resulting extracts were cleared by centrifugation and assayed for luciferase and β-galactosidase activities (*9*). β-galactosidase activity was used to correct for transfection efficiencies. Normalized luciferase activities of at least six independent experiments were used to calculate mean relative light units (RLUs) ± SEM.

5. Staining for β-galactosidase activity

Back skin of embryos of various ages was prepared using fine forceps and mounted on Nuclepore membranes (Whatman). Fixation was done for 1 to 2 hours in 1% formaldehyde + 0.2% glutaraldehyde. After washing in PBS with 0.05% BSA, skin samples were incubated with staining solution containing X-Gal as a substrate for several hours.

6. Analysis of hair follicle density

Hair follicle density of 4-week-old mice was determined by counting the number of hair shafts and/or follicles per square millimeter using a Zeiss dissecting and a Zeiss light

microscope. To determine the composition of the hair coat of wildtype and moderately affected transgenic mice, hair was plucked and single hair shafts were sorted according to characteristic structural features.

Notes
Supplementary Online Material Note 1
The groundbreaking first attempt of a theoretical explanation of biological pattern formation by Turing postulated an inhibitor and an activator as the biochemical agents that generate and manifest patterns (*10*). According to Turing's hypothesis, pattern formation is accomplished via positive and negative feedback regulation of an activator/inhibitor pair. Together with a faster diffusion and decay of the inhibitor as compared to the activator, a regular pattern is obtained (*1*).

Since then, reaction-diffusion (RD) systems have been used to model a variety of biological patterns (*1, 11, 12*). Fundamental work by Nagorcka and colleagues demonstrated that many aspects of hair follicle distribution and patterning of the developing follicle and hair shaft could be explained, in principle, on the basis of RD systems (*13-17*). Likewise, the digital hormone model of Jiang et al. which simulates the formation of feather arrays took advantage of a RD mechanism (*18*). However, most approaches lacked a concrete biochemical basis due to limited biological knowledge and experimental possibilities at that time.

Supplementary Online Material Note 2
During hair placode formation, *Wnts 3*, *4*, *6*, *7a*, *7b*, *10a*, *10b*, and *16* are expressed in the developing epidermis, whereas *Wnts 5a* and *11* are expressed in the dermis (*19*). *Wnt10b* expression is almost restricted to the hair placode; likewise, *Wnts 4*, *6*, *7b*, and *10a* are slightly up-regulated in the placode. In the outgrowing hair follicle bud, *Wnt5a* expression marks the dermal condensate and papilla, respectively; the hair matrix and the developing inner root sheath express *Wnts 10a* and *10b*. This may indicate that these three *Wnts* play the most important role during hair follicle induction. At more mature stages, the hair follicle strongly expresses a variety of *Wnt* genes all of which show a distinct pattern in the proximal follicle. These results of Reddy et al. (*19*) are summarized in fig. S1A. Initially, strong canonical WNT signaling is evident in the forming placode (fig. S1B); at advanced stages of development, strong pathway activation has switched to the dermal condensate and papilla, respectively (fig. S1B). In the almost mature follicle, canonical WNT signaling is strongest in the hair cortex, but also detectable in the dermal papilla and the adjacent hair matrix (fig. S1B). Of note, strong WNT signaling is always associated with the proximal part of the developing and mature hair follicle as it has been observed for *Wnt* gene expression.

Wnts also play important and diverse roles during feather morphogenesis (*20, 21*). In addition, signaling molecules such as BMPs, SHH, and FGFs are key regulators of follicle formation (*22, 23*). Likewise, further signaling pathways involving BMPs, SHH, and ectodysplasin participate in hair follicle formation (reviewed in (*24*)). Despite extensive research, the interconnection of these pathways during hair follicle induction and development is still a matter of debate. However, although distinct hair follicle types differ with respect to the molecular requirements for their formation, canonical WNT signaling is essential for the induction of all follicle types and appears to be the most upstream regulator of hair follicle morphogenesis (*24, 25*).

Does the WNT pathway fit the requirements of the RD mechanism (SOM text 1)? Clearly, molecular signals must precede any morphological alterations as it has been demonstrated for WNT signaling and hair placode formation (*25*). WNTs directly control *Dkk1* expression and recent reports suggest a possible autocatalyzing action through ectodysplasin or sonic hedgehog (*19, 25-28*). Furthermore, WNTs and their inhibitors are secreted into the

extracellular space where they diffuse and can act over long distances (*2, 29-32*), although measurements of diffusion rates are not available. However, WNT proteins are about 20 to 60% larger than DKKs (UniProt), and hence WNTs should diffuse more slowly. Here, we ignore possible effects of active transport, binding to extracellular components, and crowding in the extracellular space which could facilitate or hinder free diffusion. In summary, the assumptions that are necessary for pattern formation in reaction-diffusion systems match well with the WNT/DKK system.

Supplementary Online Material Note 3

In order to manipulate endogenous signaling processes, transgenic approaches with their intrinsic facility of quantitation offer the most promising strategy. Since transgene expression could be directed either to the epidermis in general or to the emerging appendages, we modeled the effects of increased activator or inhibitor expression in the epidermis and appendages, respectively, using RD-type equations reflecting characteristic features of the WNT signaling pathway. Particularly, we accounted for the non-competitive inhibition of WNT signaling by DKK. Emerging appendages correspond to zones of maximal activator production in the model. Because hair follicle induction is known to occur in several waves (*33*), we performed computer simulations for both the initial as well as for a subsequent wave when new appendages arise in between previously induced follicles.

Supplementary Online Material Note 4

In contrast to endogenous *Dkk* gene activity, transgenic inhibitor expression is independent from the WNT signaling pathway. Moreover, strong inhibitor expression in developing hair follicles is expected to make follicles largely insensitive to canonical WNT signals. In order to account for this scenario, we performed simulations of a subsequent wave in the presence of insensitive follicles that were generated during a previous inductive wave. Insensitivity means that inhibitor and activator expression by already established appendages is independent of alterations of activator and inhibitor distribution due to the induction of new follicles.

Supplementary Online Material Note 5

For transgenic perturbation of endogenous signaling, the previously described *Foxn1* promoter is the best available choice at present (*6*); although activity is not absolutely restricted to the follicle, it is much stronger in the follicle than in the epidermis (*6*) (fig. S2). As indicated by the computational modeling, weak expression in the epidermis is unlikely to disturb the effects of follicular expression. The *Foxn1* promoter is activated in the epidermis concomitant with the onset of epidermal differentiation and the induction of guard hair follicles (Fig. 3A, fig. S2). Epidermal expression reaches its maximum at the time point of first awl hair follicle induction. Follicular expression starts to exceed epidermal expression at about E17.5 (fig. S2).

Since the predicted consequence of transgenic over-expression of inhibitor is strongly dependent on the level of suppression obtained, we generated a series of transgenic mouse lines expressing *Dkk1*, *Dkk2*, and *Dkk4*, all of which are functional inhibitors of WNT signaling (*34-36*), under the *Foxn1* promoter. Transgenic effects appeared to be independent of the inhibitor's identity (Fig. 4 and fig. S5); however, the observed phenotypes were most stable for Foxn1::Dkk2 mice (i.e. almost no phenotypic variation among animals of a given line). Within developing and mature follicles, we could not detect any differences regarding the localization of gene expression and WNT signaling among wildtype and transgenic mice which is in line with the normal morphology of transgenic follicles and hair shafts.

Supporting Online Material Note 6

Since we noticed an increase of the overall hair follicle density during embryonic development (fig. S3, A and B), we addressed its possible determination using our reaction-diffusion model. Without changing distinct parameters of the equations, interfollicular distances are invariant and hair follicle numbers can only increase indirectly via the enlargement of the skin surface. Computer simulations show that follicular density increases in the presence of enhanced activator production (fig. S3C). Likewise, interfollicular distances decrease if either the inhibitor's decay is elevated or its production is reduced (fig. S3C). Indeed, *Dkk4* expression in prospective epidermal appendages appears to decrease during embryogenesis (fig. S4). Furthermore, since the developing hair follicle is a rich source of *Wnt* expression (*19*) (fig. S1), it is possible that the overall WNT level increases during embryogenesis. Thus, our simulations suggest that the activator/inhibitor pair WNT/DKK may also control the natural increase of follicle density during development.

Supplementary Online Material Note 7

To experimentally test whether follicle clusters form during an otherwise normal morphogenetic program as opposed to the postnatal development of super-numerous hair follicles in β-catenin transgenic animals (*37*), we investigated hair follicle induction throughout embryogenesis and early postnatal life. Initially, progression of morphogenesis was normal in transgenic mice (fig. S6). Hair follicle cluster formation was unequivocally observed at the time of zigzag hair follicle induction around birth (Fig. 4D, fig. S6). However, the advanced stage of some follicles that cluster around founder follicles at E18.5 suggests that cluster formation already starts earlier (fig. S6). Since awl hair induction seems to occur in two distinct waves (Fig. 3B), it is possible that the second wave of awl hair formation at about E17.5 initiates cluster emergence. At this time, strong transgene expression becomes evident in follicles (fig. S2). Indeed, the distribution of WNT signal-receiving cells confirmed the initiation of cluster formation as early as E17.5 (Fig. 4C). Of note, we did not observe follicle formation after the normal end of induction. Thus, hair follicle clusters in Foxn1::Dkk2 mice are not generated by the induction of super-numerous appendages but by follicular misdistribution during an otherwise normal morphogenesis.
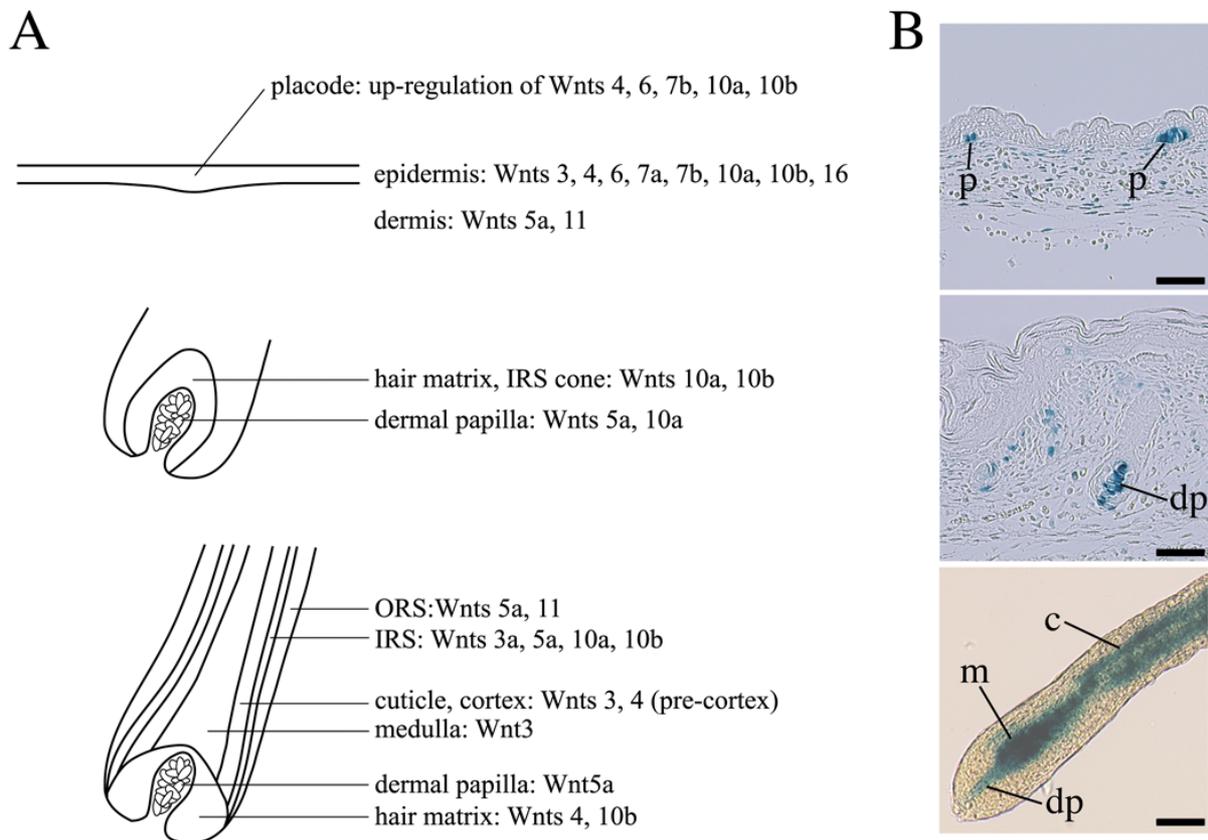
A

placode: up-regulation of Wnts 4, 6, 7b, 10a, 10b

epidermis: Wnts 3, 4, 6, 7a, 7b, 10a, 10b, 16

dermis: Wnts 5a, 11

hair matrix, IRS cone: Wnts 10a, 10b

dermal papilla: Wnts 5a, 10a

ORS:Wnts 5a, 11

IRS: Wnts 3a, 5a, 10a, 10b

cuticle, cortex: Wnts 3, 4 (pre-cortex)

medulla: Wnt3

dermal papilla: Wnt5a

hair matrix: Wnts 4, 10b

B

p   p

dp

c

m

dp

Fig. S1. Localization of *Wnt* gene expression and WNT signaling in developing hair follicles. (A) Schematic of *Wnt* gene expression in the outgrowing and more mature hair follicle summarizing the results of Reddy et al. (*19*). (B) Canonical WNT signaling in outgrowing and mature hair follicles. The activated pathway was visualized by lacZ staining of developing skin and whole mount lacZ staining of hair follicles of BATgal mice, respectively. c, cortex; dp, dermal papilla; m, matrix; p, placode. Bars, 50 μm.
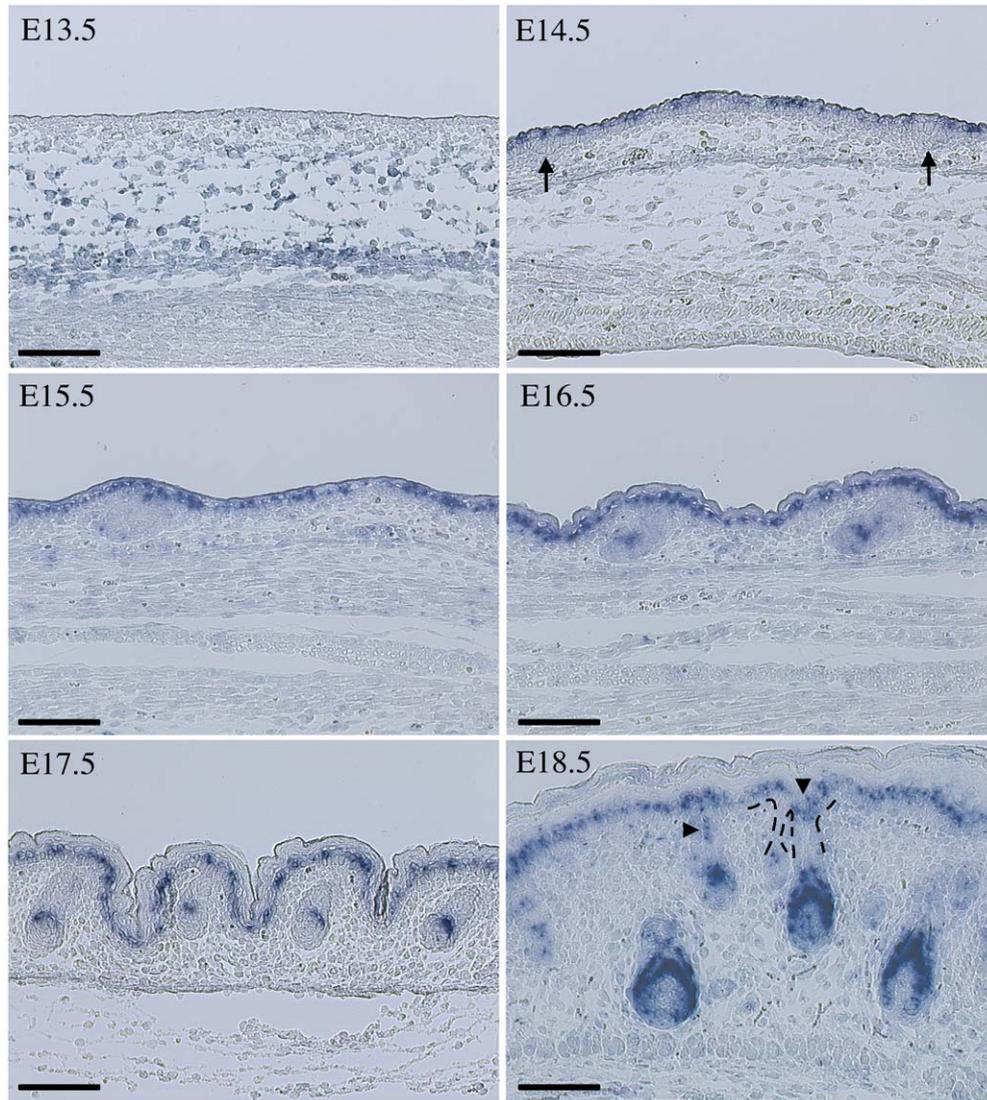
Fig. S2. The *Foxn1* promoter is concomitantly activated with the onset of epidermal stratification and hair follicle induction during mouse embryogenesis. Promoter activity was addressed by non-radioactive in situ hybridization for *Dkk2* on back skin sections of Foxn1::Dkk2 embryos of the indicated age. Forming hair placodes are marked by arrows. Note that, finally, expression in the follicle significantly exceeds epidermal gene activity. By contrast, transgene expression in the interfollicular epidermis and the infundibulum (arrowheads) is indistinguishable. The dashed lines marking the epidermal-dermal border highlight the fact that infundibuli of follicles within a cluster are often not fused. Bars, 100 μm.
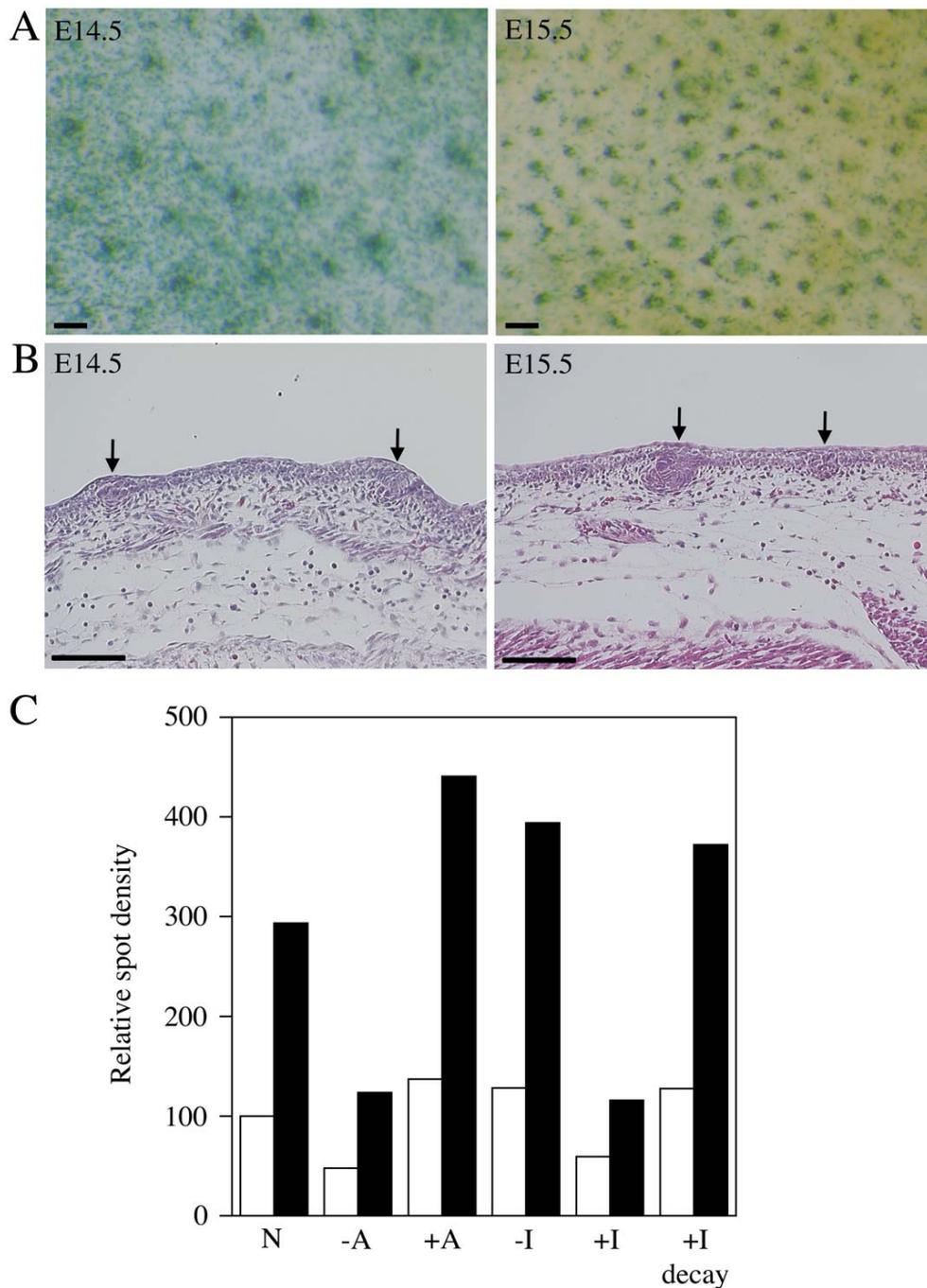
Fig. S3. Hair follicle density increases during embryonic development. (A) In BATgal skin, the density of lacZ-positive cell clusters that are associated with forming hair follicles (see Fig. 1A) increases during embryonic development. Top views of representative whole mount stainings are shown. Bars, 100 μm. (B) The increase of hair follicle density during embryonic development is also visible on hematoxylin and eosin stained sections of back skin of the indicated ages. Follicles are marked by arrows. Bars, 100 μm. (C) Modeling of the effects of altered activator (A) and inhibitor (I) production, respectively, as well as of increased inhibitor decay using our model demonstrates significant changes in spot density of the respective activator plots. Relative densities after the first (white) or the second (black) wave were calculated, whereby the density for our standard conditions (N) was set to 100 for the first wave.
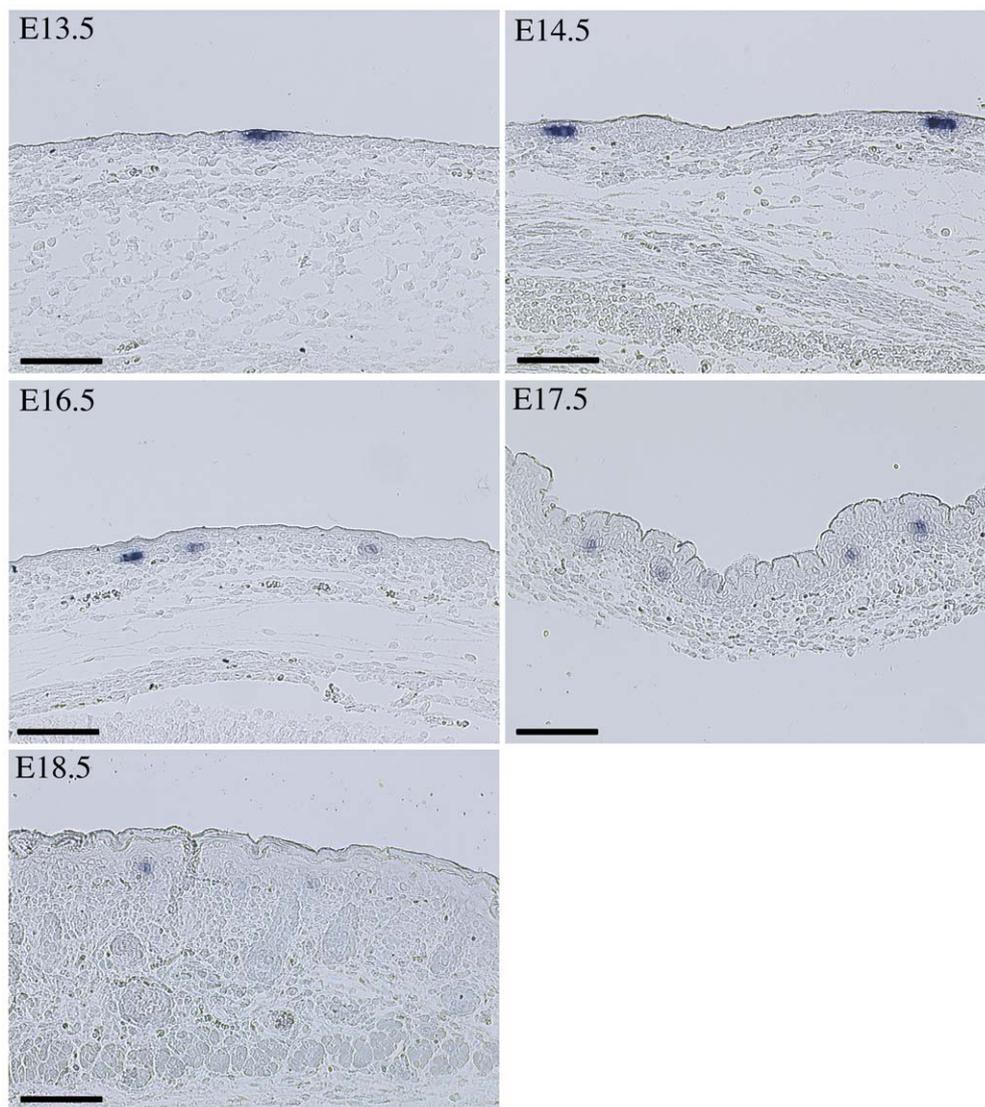
Fig. S4. Hair follicle induction-associated *Dkk4* expression decreases during embryonic development of mice. Gene expression was addressed by non-radioactive in situ hybridization of back skin sections. Bars, 100 μm.
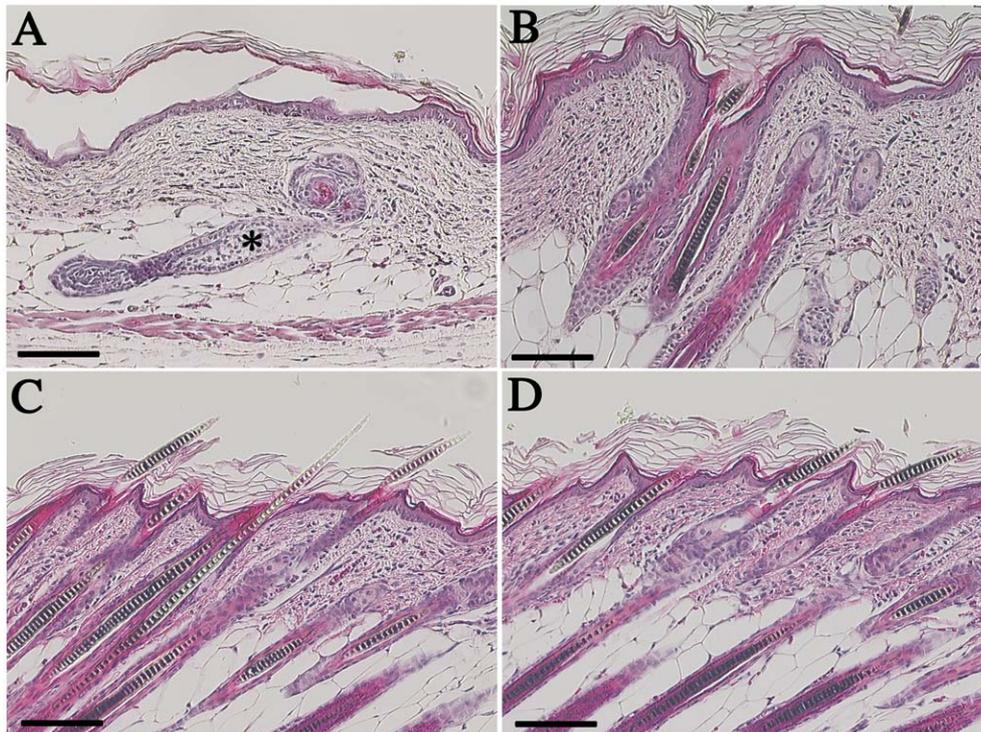
Fig. S5. Transgenic *Dkk1* expression gives rise to hair follicle clustering. Back skin of 10-day-old Foxn1::Dkk1 mice was stained with hematoxylin and eosin. After backcrossing to BALB/c mice, the nude phenotype of strongly affected transgenic animals was converted to a variable appearance of mice and of distinct areas on a single mouse. Whereas nude patches (A) exclusively contain aberrant guard hair follicles (*), hairy areas (B-D) are characterized by different levels of clustering. Bars, 100 μm.
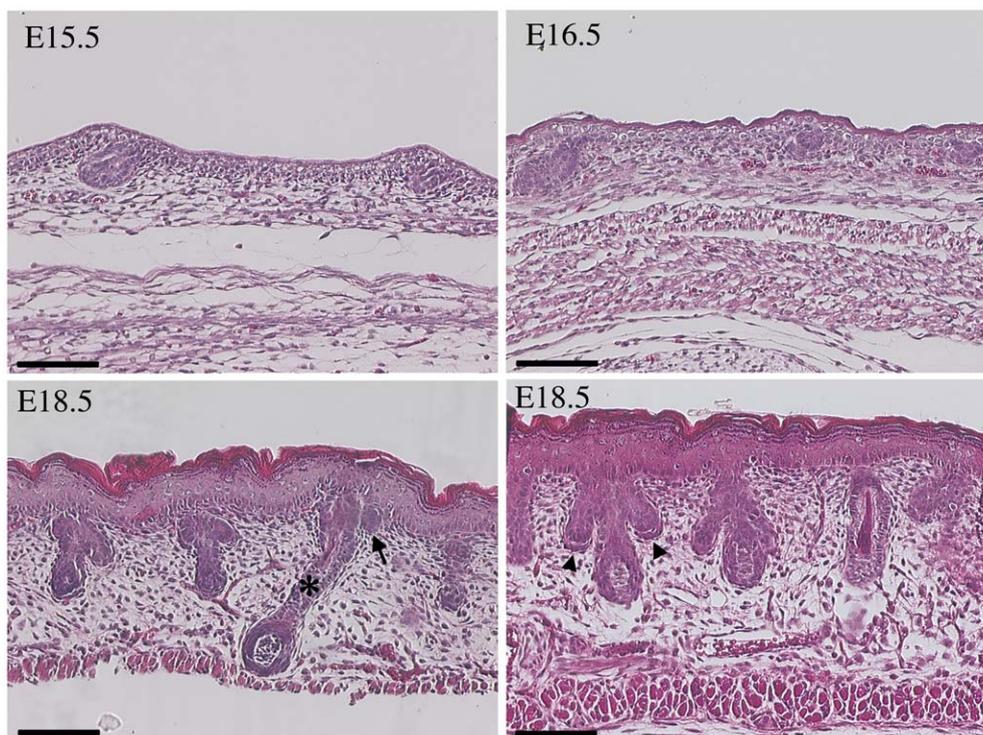
Fig. S6. Hair follicle induction during embryonic development in Foxn1::Dkk2 mice. Back skin of the indicated age was stained with hematoxylin and eosin. Whereas hair follicle formation appears to be normal during the first waves of induction (top), cluster formation is evident at the time of first zigzag hair follicle induction at E18.5 (bottom). Clearly, guard hair follicles (*) take part in cluster formation (arrow). New follicles can be simultaneously induced in a single cluster (arrowheads) as suggested by our simulations (Fig. 2B). The advanced stage of developing hair follicles (arrowheads) that cluster around the founder follicle at E18.5 indicates that formation of clusters may already start during the last wave of awl hair follicle induction at about E17-E17.5. Infundibuli of marked hair follicles (arrow and arrowheads, respectively) are not fused to that of the founding members of their respective clusters. Bars, 100 μm.

References
1. A. J. Koch, H. Meinhardt, *Rev Mod Phys* **66**, 1481 (1994).
2. C. Y. Logan, R. Nusse, *Annu Rev Cell Dev Biol* **20**, 781 (2004).
3. A. Cornish-Bowden, *Fundamentals of Enzyme Kinetics* (Portland Press Ltd, 2004), pp.
4. J. D. Murray, *Mathematical Biology* (Springer Verlag, Berlin, 1993), pp.
5. S. Maretto *et al.*, *Proc Natl Acad Sci U S A* **100**, 3299 (2003).
6. T. Schlake, *Development* **132**, 2981 (2005).
7. N. Weger, T. Schlake, *J Invest Dermatol* **125**, 873 (2005).
8. S. Mizushima, S. Nagata, *Nucleic Acids Res* **18**, 5322 (1990).
9. T. Schlake, M. Schorpp, M. Nehls, T. Boehm, *Proc Natl Acad Sci USA* **94**, 3842 (1997).
10. A. Turing, *Philos Trans R Soc Lond B* **237**, 37 (1952).
11. A. Gierer, H. Meinhardt, *Kybernetik* **12**, 30 (1972).
12. A. Garfinkel, Y. Tintut, D. Petrasek, K. Bostrom, L. L. Demer, *Proc Natl Acad Sci U S A* **101**, 9247 (2004).
13. B. N. Nagorcka, J. R. Mooney, *J Theor Biol* **98**, 575 (1982).
14. B. N. Nagorcka, *Biosystems* **16**, 323 (1983).
15. B. N. Nagorcka, J. R. Mooney, *IMA J Math Appl Med Biol* **9**, 249 (1992).
16. B. N. Nagorcka, *Aust J Agric Res* **46**, 333 (1995).
17. B. N. Nagorcka, *Aust J Agric Res* **46**, 357 (1995).
18. T. X. Jiang *et al.*, *Int J Dev Biol* **48**, 117 (2004).
19. S. Reddy *et al.*, *Mech Dev* **107**, 69 (2001).
20. C. H. Chang *et al.*, *Mech Dev* **121**, 157 (2004).
21. R. Chodankar *et al.*, *J Invest Dermatol* **120**, 20 (2003).
22. H. S. Jung *et al.*, *Dev Biol* **196**, 11 (1998).
23. S. A. Ting-Berreth, C. M. Chuong, *Dev Dyn* **207**, 157 (1996).
24. R. Schmidt-Ullrich, R. Paus, *Bioessays* **27**, 247 (2005).
25. T. Andl, S. T. Reddy, T. Gaddapara, S. E. Millar, *Dev Cell* **2**, 643 (2002).
26. A. Niida *et al.*, *Oncogene* **23**, 8520 (2004).
27. M. N. Chamorro *et al.*, *Embo J* **24**, 73 (2005).
28. J. Huelsken, R. Vogel, B. Erdmann, G. Cotsarelis, W. Birchmeier, *Cell* **105**, 533 (2001).
29. V. L. Church, P. Francis-West, *Int J Dev Biol* **46**, 927 (2002).
30. V. A. Schneider, M. Mercola, *Genes Dev* **15**, 304 (2001).
31. M. Strigini, S. M. Cohen, *Curr Biol* **10**, 293 (2000).
32. C. J. Neumann, S. M. Cohen, *Development* **124**, 871 (1997).
33. F. W. Dry, *J Genet* **16**, 287 (1926).
34. A. Glinka *et al.*, *Nature* **391**, 357 (1998).
35. B. Mao, C. Niehrs, *Gene* **302**, 179 (2003).
36. V. E. Krupnik *et al.*, *Gene* **238**, 301 (1999).
37. U. Gat, R. DasGupta, L. Degenstein, E. Fuchs, *Cell* **95**, 605 (1998).